

A novel ultrasonic method for measuring breast density and breast cancer risk

Carri K. Glide-Hurst^{*a}, Neb Duric^b, Peter J. Littrup^b

^aWilliam Beaumont Hospital, 3601 W. Thirteen Mile Rd., Royal Oak, MI USA 48073;

^bKarmanos Cancer Institute, 4100 John R. Street, 5 HWCRC, Detroit, MI USA 48201

ABSTRACT

Women with high mammographic breast density are at 4- to 6-fold increased risk of developing breast cancer compared to women with fatty breasts. However, current breast density estimations rely on mammography, which cannot provide accurate volumetric breast representation. Therefore, we explored two techniques of breast density evaluation via ultrasound tomography. A sample of 93 patients was imaged with our clinical prototype; each dataset contained 45-75 tomograms ranging from near the chest wall through the nipple. Whole breast acoustic velocity was determined by creating image stacks and evaluating the sound speed frequency distribution. Ultrasound percent density (USPD) was determined by segmenting high sound speed areas from each tomogram using k-means clustering, integrating over the entire breast, and dividing by total breast area. Both techniques were independently evaluated using two mammographic density measures: (1) qualitative, determined by a radiologist's visual assessment using BI-RADS Categories, and (2) quantitative, via semi-automatic segmentation to calculate mammographic percent density (MPD) for craniocaudal and medio-lateral oblique mammograms. ~140 m/s difference in acoustic velocity was observed between fatty and dense BI-RADS Categories. Increased sound speed was found with increased BI-RADS Category and quantitative MPD. Furthermore, strong positive associations between USPD, BI-RADS Category, and calculated MPD were observed. These results confirm that utilizing sound speed, both for whole-breast evaluation and segmenting locally, can be implemented to evaluate breast density.

Keywords: Breast density, ultrasound tomography, transmission ultrasound, tissue characterization, breast cancer risk

1. INTRODUCTION

Emerging evidence has shown that women with high mammographic breast density are at 4 to 5-fold increased risk of developing breast cancer.¹ Furthermore, increased breast density has been shown to be more prognostic of overall breast cancer risk than nearly all other risk factors.²⁻⁴ However, current breast density estimation relies on radiologists' visual assessment of mammograms using the four-category Breast Imaging Reporting and Data System (BI-RADS) lexicon. This subjective classification has obvious limitations due to reported intra- and inter-reader variability.⁵ Further, a mammogram is a 2-D projection that cannot provide an accurate volumetric estimate of the density due to the breast thickness not being taken into account. Presumably, breast cancer risk would be more strongly related to the *volume* of dense tissue as opposed to the projected area. To this end, efforts have been made to estimate volumetric breast density through computational modeling, evaluating whole-breast MRI sequences, and calibrating screen-film images with step wedges. The volumetric measure that we are presenting, however, is novel due to using ultrasound tomography transmission images (i.e. sound speed) to provide estimates of volumetric breast density. Perhaps the most remarkable characteristic of breast density is the fact that it can be modified. This is significant because many contributing factors for breast cancer risk (i.e. age, family history) cannot be changed. Because breast density *can* be altered, it has been suggested for use as a surrogate marker⁶, intermediate phenotype for breast cancer⁷, and indicator for monitoring potential preventive⁸ or therapeutic strategies⁹. These considerations suggest that finding new techniques to quantify breast density is particularly advantageous.

*Carri.Glide-Hurst@beaumont.edu; phone 1 248 551-7479

2. METHODOLOGY

2.1 Imaging device

The principles of CURE, or Computerized Ultrasound Risk Evaluation, operation and image reconstruction have been described in detail elsewhere¹⁰, although a brief overview is outlined here. The patient is positioned prone with the breast suspended in a water tank. The water, with well-defined sound speed properties, serves as both the coupling medium and matching layer between the breast tissue and the surrounding 20 cm diameter ring transducer. The transducer operates at a frequency of 1.5 MHz, scanning from near the chest wall through the nipple region, with each dataset containing 45-75 sound speed tomograms. The absolute sound speed measurements (in m/s) are based on the signals transmitted through the breast tissue. Absolute calibration is possible because the arrival times of the transmitted signal are compared to water, whose sound speed is known at the time and temperature of the scan.

2.2 Patient population

The patients imaged with our clinical prototype were recruited from the Walt Comprehensive Breast Center located at Karmanos Cancer Institute, with all imaging procedures performed under an Institutional Review Board approved protocol and in compliance with the Health Insurance Portability and Accountability Act. The patient population included 93 case sets and provided a variety of breast shapes and densities, with a mean age of 48.2 years (range: 21-85).

2.3 Ultrasonic breast density measures

2.3.1 Whole breast acoustic velocity

Whole breast acoustic velocity was determined by creating image stacks for each patient's breast. Because an image stack corresponds to the entire breast volume, the histograms represent the statistical distribution of all sound speed voxels within that breast. Each sound speed frequency distribution was analyzed to determine the overall mean sound speed value, resulting in a single-valued estimate of the average sound speed representative of the whole breast

2.3.2 Ultrasound percent density (USPD)

High sound speed regions (i.e. dense parenchyma) were segmented for each tomogram, and the total number of dense voxels was calculated as the integration of high sound speed region areas over the entire breast volume. Similarly, the total breast area was estimated for each tomogram, and the voxels were summed over all slices in the breast (~45-75 tomograms). If we define a as the first slice near the chest wall, b as the final slice in the image stack at the nipple region, A_D as the dense region of high sound speed, determined using k-means clustering, for that particular slice, and A as the total breast area for that slice, the volumetric ultrasound percent density (USPD) can be calculated using the following equation:

$$\text{USPD (\%)} = \frac{\sum_{n=a}^b A_D}{\sum_{n=a}^b A} \times 100 \%$$

2.4 Mammographic percent density (MPD) evaluation

Both ultrasound techniques were evaluated using two mammographic density measures: (1) qualitative, as determined by a radiologist's visual assessment using BI-RADS Categories (the current standard of care) and (2) quantitative, via digitization and semi-automatic segmentation of craniocaudal and medio-lateral oblique mammograms (MPD).

2.4.1 BI-RADS Category analysis

As an independent evaluation of our ultrasound tomography approaches, we compared our results to the current standard of care for breast density analysis: BI-RADS Categories. A board-certified radiologist with over 10 years of mammography experience examined the mammograms corresponding closest to the CURE exam date, and assigned each patient into a BI-RADS compositional category of: 1. almost entirely fat (<25% glandular), 2. scattered (25-50%

glandular), 3. heterogeneously dense (51-75% glandular) and 4. extremely dense (>75% glandular). The resulting population distribution is shown in Table 1.

Table 1: The BI-RADS compositional category distribution for the patient population.

BI-RADS Compositional Category	Patient Sample (% of population)
1: Fatty (< 25%)	11 (12%)
2: Scattered (26 - 50%)	60 (65%)
3: Heterogeneous (51 - 75%)	16 (17%)
4: Dense (> 75%)	6 (7%)

A one-way ANOVA tested for significant differences between for our ultrasound measurements between BI-RADS Categories, and a Spearman correlation coefficient was calculated to determine strength of association.

2.4.2 Quantitative mammographic percent density

To determine a more quantitative comparison of MPD, archival mammograms in the craniocaudal (CC) and mediolateral (MLO) projections were digitized with a Vidar VXR-16 Dosimetry Pro digitizer using a TWAIN interface (version 5.2.1) with the following parameters: logarithmic translation table, 71 dpi resolution, and an 8-bit depth. A segmentation routine for breast density evaluation, described in detail elsewhere¹¹, was implemented to segment the glandular from total breast area. Finally, we compared the USPD to calculated MPD for both CC and MLO views, and corresponding associations between the variables were determined.

3. RESULTS

3.1 Whole breast acoustic velocity

Approximately 140 m/s difference in acoustic velocity was found between the fatty and dense BI-RADS Categories, with statistically significant differences in mean sound speed demonstrated between *each* category (ANOVA, $\alpha = 0.05$). An overall statistically significant strong positive correlation (Spearman $\rho = 0.73$, $p < 0.001$) was observed between the mean sound speed and BI-RADS category, as shown by the boxplot in Figure 1(left). The mean sound speed measurement for BI-RADS category 1 (fatty) patients was 1388.4 +/- 7.4 m/s, whereas for dense breasted patients, the value was 1532.2 +/- 23.6 m/s. This analysis revealed that detectable sound speed changes according to BI-RADS category were achieved. This is an important result because it shows that our methods were consistent with the current standard of care.

However, the relationship between BI-RADS category and sound speed demonstrates limited clinical applicability because of the wide range of sound speed values for each breast density category. Wide variations in measurement can be attributed to several factors, including the coarseness of BI-RADS categories, the subjectivity involved in the radiologist's visual assessment, limited sample numbers, and the single measurement available for each patient. To further address this, we investigated the direct comparison of sound speed with calculated mammographic density, to determine if a continuous sound speed scale may be more informative than the coarse scale currently used in the BI-RADS 4-category lexicon. Moderately strong positive associations were demonstrated between mean acoustic velocity and quantitative measures of mammographic percent breast density for both MLO and CC views ($r^2 = 0.65-0.76$), respectively. Figure 1(right) shows the sound speed according to quantitative mammographic percent density estimates for the CC view. Similar results were observed for the MLO view (not shown).

Figure 1 (right) shows that whole breast acoustic velocity results exhibited an asymptotic minimum threshold representing a baseline sound speed for fattier breasts. The data revealed that breast sound speed stayed relatively constant over the range of 0 to ~40% MPD. This result was consistent with the results demonstrated in Figure 1 (left)

that compared sound speed to BI-RADS category. It seems likely that for fatty breasts (i.e. MPD < 40%), lower sound speed values caused by the predominance of fatty tissue may strongly influence the global sound speed of the breast. Further, it is also possible that smaller amounts of fibroglandular tissue are not readily identified due to the relatively low resolution of sound speed images. Having improved resolution in future reconstruction algorithms may allow this type of analysis to be more sensitive to smaller fibroglandular tissue quantities. Nevertheless, breast sound speed appears to be a sensitive predictor of mammographic density in women with mammographic density greater than 40%, even with this limited patient sample. This is an important result because our methods appear to be most sensitive at the higher breast densities, where the associated breast cancer risk is also the greatest.

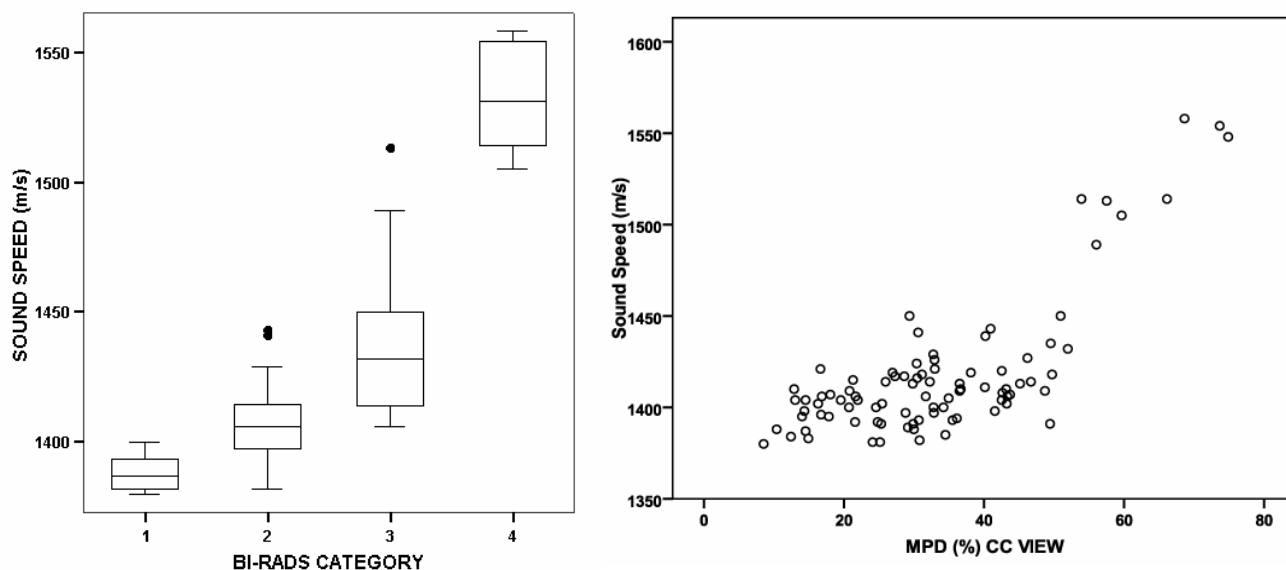


Fig. 1. (Left) Box-plot of mean sound speed value for 93 patients categorized by BI-RADS compositional category. The differences in mean sound speed for every category was significant using a one-way ANOVA and Scheffé post-hoc analysis. (Right) A comparison of the mean sound speed measurement with quantitative mammographic percent density for the CC view. A strong positive association was observed, with similar results for the MLO view (not shown).

3.2 USPD

As a comparison to the current standard of care for breast density analysis, we compared the USPD to BI-RADS Categories, and the results are summarized by the boxplot in Figure 2. In general, a strong positive association was observed between USPD and BI-RADS Category (Spearman $\rho = 0.69$, $p < 0.001$). A one-way analysis of variance revealed that a significant difference existed between the mean USPD among BI-RADS Categories ($p < 0.01$). Further post hoc analyses using the Scheffé criterion indicated that significant differences in mean USPD were observed between each BI-RADS Category ($\alpha = 0.05$). Most notably, the difference in USPD between BI-RADS 1 (fatty) and BI-RADS 4 (dense) was $\sim 40\%$. This is a critical result because it shows that there is a substantial change in USPD between women in the highest breast cancer risk category compared to those in the lowest category (and hence, lowest risk).

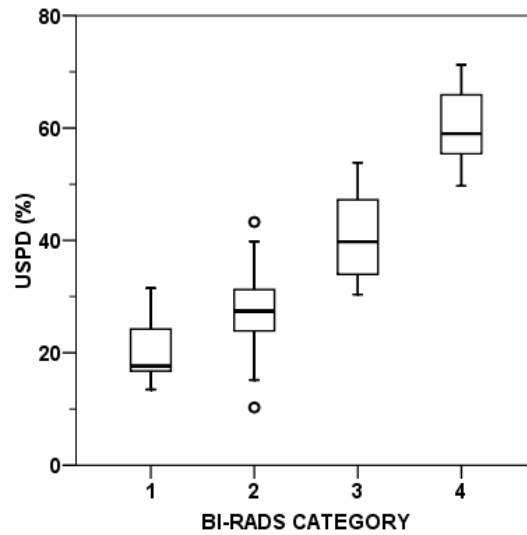


Fig. 2. Boxplot showing the strong correlation (Spearman $\rho = 0.69$ ($p < 0.001$)) between the USPDP and BI-RADS compositional category. The differences between all BI-RADS Categories were found to be significant, demonstrating the agreement of the USPDP technique with the current standard of care.

To further validate our approach, we compared USPDP to calculated mammographic percent density for both CC and MLO mammographic views. Figure 3(A) shows the results for the CC view. Because comparisons were made between volumetric (USPDP) and area (MPD) measures, curve fitting was used to take this into account in a manner similar to what has been previously applied to MRI breast density analysis.¹² If we assume a simplified case with a dense tissue spherical volume embedded in a spherical shell of fatty tissue, the volume (i.e. USPDP) would be proportional to the projected area (MPD) to the 3/2 power. Figure 3(B) demonstrates the results with this 3/2 fit applied. Moderate to strong positive correlations were observed between percent area and percent volume for both CC and MLO (not shown) views ($r^2 = 0.75$ and 0.59 , respectively).

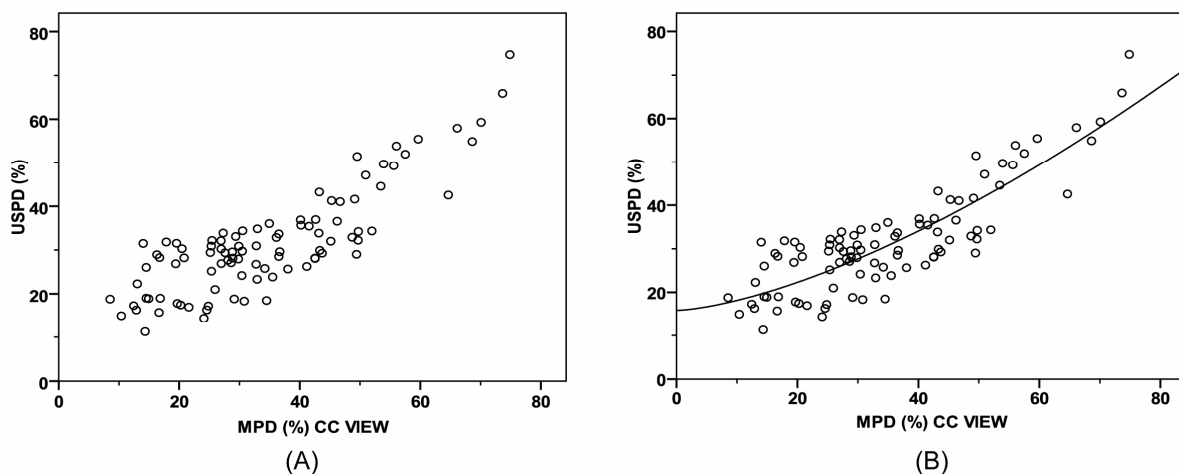


Fig. 3. (A) Comparison of ultrasound percent density (USPDP) and quantitative mammographic percent density (MPD), showing the strong positive association between the variables. (B) Volume to area fit for the CC mammographic view (Pearson $r = 0.75$)

3.3 Ultrasound Mammogram

Furthermore, by performing an average intensity summation of different projections, creating an ultrasound tomography “mammogram” and further segmentation of high sound speed regions is possible, as shown in Figure 4. Also shown is the corresponding patient mammogram, where the distribution of fatty and fibroglandular tissue is apparent.

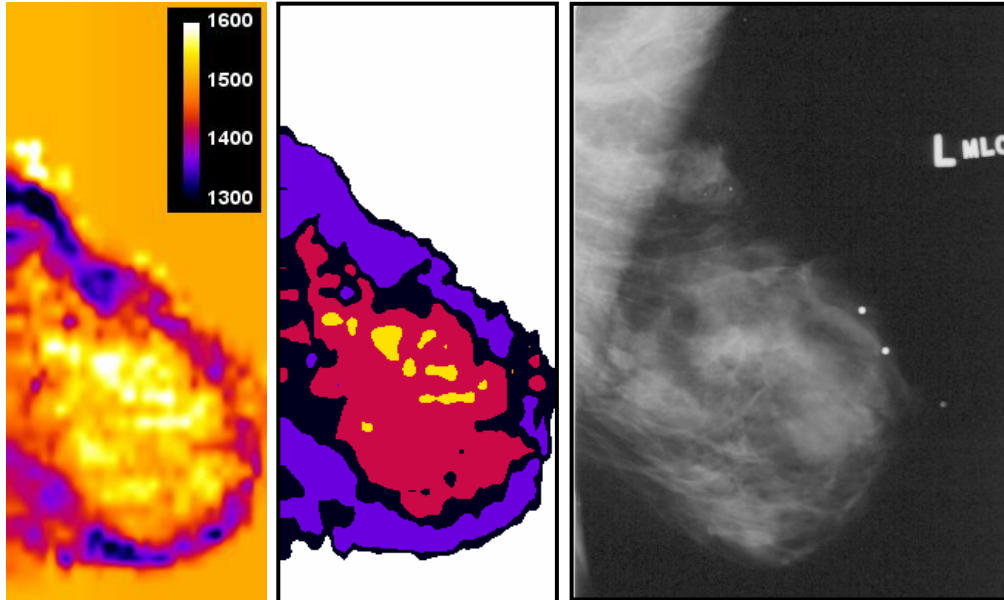


Fig. 4. (Left) Sound speed projected cross section with sound speed (m/s) shown in the scale, (center) segmented sound speed cross section, and (right) corresponding MLO mammogram for the same patient. Note the distribution of high sound speed regions (i.e. 1500+ m/s) corresponds well to the distribution of fibroglandular tissue on the mammogram.

3.4 Tomographic approach

Having cross-sectional tomograms introduces the potential of providing volumetric estimates in lieu of projected areas currently provided by mammography. However, using mammographic projections to estimate dense tissue regions does not take into account the three-dimensional deformation and displacement of breast tissues caused by compression plates. This is one distinct advantage of using our volumetric breast density estimates. Presumably, breast cancer risk would be more strongly associated with the volume of dense tissue as opposed to the projected area. Comparisons between CT and mammography revealed that contrast in breast images is strongly related to the presence of overlying tissue obscuring structures⁹¹. Clearly this is a significant disadvantage for mammography, which collapses all of the volumetric information into two dimensions. Because our ultrasound tomography technique allows us to assess cross-sectional tomograms, we are better able to evaluate the distribution of fatty and glandular tissue on a slice by slice basis than currently possible with mammography. Being able to investigate different cross sections of the breast eliminates the effects that surrounding tissue may have on decreasing image contrast.

4. CONCLUSION

We have developed and evaluated two methodologies to implement ultrasound tomography methods for breast density evaluation. Both whole-breast acoustic velocity and segmented USPD correlate strongly with the current standard for care (BI-RADS Categories) and calculated mammographic percent density. Therefore, these results demonstrate the feasibility of using ultrasound tomography for breast density analysis, offering a safer and noninvasive approach to evaluating breast density, which can be a valuable measure of breast cancer risk.

REFERENCES

- [1] Santen, R. J. and Mansel, R., "Benign breast disorders," *N Engl J Med* **353**, 275-285 (2005).
- [2] Barlow, W. E., White, E., Ballard-Barbash, R., Vacek, P. M., Titus-Ernstoff, L., Carney, P. A., Tice, J. A., Buist, D. S., Geller, B.M., Rosenberg, R., Yankaskas, B.C., and Kerlikowske, K., "Prospective breast cancer risk prediction model for women undergoing screening mammography," *J Natl Cancer Inst* **98**, 1204-1214 (2006).
- [3] Boyd, N. F., Lockwood, G. A., Byng, J. W., Tritchler, D. L., and Yaffe, M. J., "Mammographic densities and breast cancer risk," *Cancer Epidemiol Biomarkers Prev.* **7**, 1133-1144 (1998).
- [4] Harvey, J. A. and Bovbjerg, V.E., "Quantitative assessment of mammographic breast density: relationship with breast cancer risk," *Radiology* **230**, 29-41 (2004).
- [5] Berg, W. A., Campassi, C., Langenberg, P., and Sexton, M.J., "Breast Imaging Reporting and Data System: inter- and intraobserver variability in feature analysis and final assessment," *Am J Roentgenol* **174**, 1769-1777 (2000).
- [6] Boyd, N. F., Martin, L. J., Li, Q., Sun, L., Chiarelli, A. M., Hislop, G., Yaffe, M. J., and Minkin, S., "Mammographic density as a surrogate marker for the effects of hormone therapy on risk of breast cancer," *Cancer Epidemiol. Biomarkers Prev.* **15**, 961-966 (2006).
- [7] Boyd, N. F., Rommens, J. M., Vogt, K. Lee, V., Hopper, J. L., Yaffe, M. J. and Paterson, A. D., "Mammographic breast density as an intermediate phenotype for breast cancer," *Lancet Oncol* **6**, 798-808 (2005).
- [8] Brisson, B. B., Cote, J., Maunsell, G., Berube, E., Robert S, J., "Tamoxifen and Mammographic Breast Densities," *Cancer Epidemiology Biomarkers & Prevention* **9**, 911-915 (2000).
- [9] Harvey, J. A., Bovbjerg, V. E., Smolkin, M. E., Williams, M. B. and Petroni, G. R., "Evaluating Hormone Therapy-associated Increases in Breast Density Comparison Between Reported and Simultaneous Assignment of BI-RADS Categories, Visual Assessment, and Quantitative Analysis(1)," *Acad Radiol* **12**, 853-862 (2005).
- [10] Duric, N., Littrup, P., Poulou, L., Babkin, A., Pevzner, R., Holsapple, E., Rama, O. and Glide, C., "Detection of breast cancer with ultrasound tomography: first results with the Computed Ultrasound Risk Evaluation (CURE) prototype," *Med Phys* **34**, 773-785 (2007).
- [11] Glide-Hurst, C., Duric, N., Littrup, P. A New Method for Quantitative Analysis of Mammographic Density. *Med. Phys.* **34**, 4491-4498 (2007).
- [12] Wei, J., Chan, H. P., Helvie, M. A., Roubidoux, M. A., Sahiner, B., Hadjiiski, L. M., Zhou, C., Paquerault, S., Chenevert, T., and Goodsitt, M. M., "Correlation between mammographic density and volumetric fibroglandular tissue estimated on breast MR images," *Med Phys* **31**, 933-942 (2004).